

# Adaptive Tuning Wavelet Neural Controller Design with a Smooth Compensator

Chun-Fei Hsu and Kuo-Hsiang Cheng

**Abstract**—In this paper, an adaptive tuning wavelet neural control (ATWNC) is proposed. The proposed ATWNC system is composed of a wavelet neural controller and a smooth compensator. The wavelet neural control is utilized to approximate an ideal controller and the smooth compensator is used to remove the chattering phenomena of conventional sliding-mode control completely. In the ATWNC, the learning algorithm is derived based on the Lyapunov function, thus the closed-loop system's stability can be guaranteed. Then, the proposed ATWNC approach is applied to a second-order chaotic nonlinear system to investigate the effectiveness. Through the simulation results, the proposed ATWNC scheme can achieve favorable tracking performance and the convergence of the tracking error and control parameters can be accelerated by the developed PI adaptation learning algorithm.

**Index Terms**—Adaptive control, neural control, chaotic system, wavelet neural network.

## I. INTRODUCTION

From the control point of view, if the exact model of the controlled system is well known, there exists an ideal controller scheme to achieve favorable control performance by canceling all the system dynamics [14]. However, a tradeoff between stability and accuracy is necessary for the performance of ideal controller. To relax this requirement, a sliding-mode control strategy offers a number of attractive properties for the tracking control, such as insensitivity to parameter variations, external disturbance rejection and fast dynamic responses [14]. However, the chattering phenomena of the sliding mode control will wear the bearing mechanism.

Recently, some intelligent control schemes like as neural network (NN)-based adaptive control have been developed [5], [7], [10], [12], [18]. The most useful property is their ability of NNs can approximate arbitrary linear or nonlinear mapping through learning. By adequately choosing neural network structures, training methods and sufficient input data, the NN-based adaptive controllers are capable to compensate for the effects of nonlinearities and system uncertainties [7]. To achieve better learning performance of NN, some researchers have combined the layered structure of NN and

the wavelet functions to construct the wavelet neural network (WNN) [1], [20]. Unlike the sigmoidal functions used in conventional neural networks, wavelet functions are spatially localized, so that the learning capability of WNN is more efficient than the conventional sigmoidal function neural network [1]. There have been many considerable interests in exploring the applications of WNN to deal with unknown nonlinearity control systems [6], [9], [15]. These WNN-based adaptive controllers combine the capability of artificial neural networks for learning ability and the capability of wavelet decomposition for identification ability.

In order to ensure the NN-based and WNN-based adaptive control systems' stability, a compensation controller could be designed to dispel the approximation error. The most frequently used of compensation controller is like a sliding-mode control, which requires the bound of the approximation error [9]. If the bound of approximation error is chosen too small, the system stabilization can not guarantee. However, if the bound of approximation error is chosen too large, the control effort will cause chattering phenomena to wear the bearing mechanism.

To tackle this problem, an approximation error bound estimation mechanism is investigated to estimate the bound of approximation error so that the chattering phenomenon of the control effort can be reduced [13]. However, the adaptive law for the estimation error bound will make it go to infinity.

This paper proposed an adaptive tuning wavelet neural control (ATWNC) system for a chaotic dynamic system. The proposed ATWNC system consists of a wavelet neural controller and a smooth compensator. The wavelet neural controller utilizes a WNN to online mimic an ideal controller using the PI type adaptation learning algorithm, and the smooth compensator uses a fuzzy system to remove the chattering phenomena on conventional sliding-mode control completely. In addition, the learning algorithm is derived based on the Lyapunov function to guaranteed system's stability and the Taylor linearization technique is employed to increase the learning ability of WNN. Finally, some simulation results are provided to verify the effectiveness of the developed ATWNC scheme.

## II. PROBLEM FORMULATION

Chaotic systems have been studied and known to exhibit complex dynamical behavior. The interest in chaotic systems lies mostly upon their complex, unpredictable behavior, and extreme sensitivity to initial conditions as well as parameter variations [3], [8], [11]. Consider a second-order chaotic dynamic system, the dynamics of Duffing's equation is

Manuscript received January 20, 2009. This work was supported in part by the National Science Council of Republic of China under grant NSC 97-2221-E-216-029.

C. F. Hsu is with the Department of Electrical Engineering, Chung Hua University, Hsinchu 300, Taiwan, Republic of China (phone: 886-3-5186399; fax: 886-3-5186436; e-mail: fei@chu.edu.tw).

K. H. Cheng is with the Mechanical and Systems Research Laboratories, Industrial Technology Research Institute, Chutung, Hsinchu 310, Taiwan, Republic of China (e-mail: KHCheng@itri.org.tw).

described as [3]

$$\ddot{x} = -p\dot{x} - p_1x - p_2x^3 + q\cos(\omega t) + u = f(\mathbf{x}) + u \quad (1)$$

where  $\mathbf{x} = [x \dot{x}]^T$  is the state vector of the system,  $t$  is the time variable;  $w$  is the frequency,  $f(\mathbf{x}) = -p\dot{x} - p_1x - p_2x^3 + q\cos(\omega t)$  is the system dynamic function,  $u$  is the control effort, and  $p, p_1, p_2$  and  $q$  are real constants. Depending on the choices of these constants, the solutions of system (1) may display complex phenomena, including various periodic orbits behaviors and some chaotic behaviors. To observe these complex phenomena, the open-loop system behavior with  $u=0$  was simulated with  $p=0.4, p_1=-1.1, p_2=1.0$  and  $\omega=1.8$ . The phase plane plots with an initial condition  $(0, 0)$  are shown in Figs. 1(a) and 1(b) for  $q=2.1$  (chaotic) and  $q=7.0$  (period 1), respectively. It is shown that the uncontrolled chaotic dynamic system has different chaotic trajectories for different values of  $q$  [3]. The control objective of chaotic system is to find a control law so that the state trajectory  $x$  can track a trajectory command  $x_c$ . A tracking error is defined as

$$e = x_c - x. \quad (2)$$

If the system dynamic function is well known, there exists an ideal controller as [14]

$$u^* = -f(\mathbf{x}) + \ddot{x}_c + k_1\dot{e} + k_2e \quad (3)$$

where the  $k_1$  and  $k_2$  are the non-zero constants. Apply the ideal controller (3) into (1), it obtains that

$$\ddot{e} + k_1\dot{e} + k_2e = 0. \quad (4)$$

If  $k_1$  and  $k_2$  are chosen to correspond to the coefficients of a Hurwitz polynomial, that is a polynomial whose roots lie strictly in the open left half of the complex plane, then it implies that  $\lim_{t \rightarrow \infty} e(t) = 0$  [14]. However, the system dynamics is always unknown; the ideal controller  $u^*$  can not be implemented.

Rewriting (1), the nominal model of the nonlinear dynamic system can be represented as follows

$$\ddot{x} = f_n(\mathbf{x}) + u \quad (5)$$

where  $f_n(\mathbf{x})$  is a mapping that represents the nominal behavior of  $f(\mathbf{x})$ . If uncertainties occur, i.e., the parameters of the system deviate from the nominal value and/or the external disturbance is added into the system, the controlled system can be modified as

$$\ddot{x} = f_n(\mathbf{x}) + \Delta f(\mathbf{x}) + u + d = f_n(\mathbf{x}) + u + z \quad (6)$$

where  $d$  is the external disturbance,  $\Delta f(\mathbf{x})$  denotes the system uncertainties, and  $z$  is called the lumped uncertainty which defined as  $z = \Delta f(\mathbf{x}) + d$  with the assumption  $|z| \leq Z$ , in which  $Z$  is a given positive constant. A sliding surface is defined as

$$s = \dot{e} + k_1e + k_2 \int_0^t e(\tau) d\tau. \quad (7)$$

The sliding-mode control law is given as [14]

$$u_{sc} = u_{eq} + u_{hr} \quad (8)$$

where the equivalent controller  $u_{eq}$  is represented as

$$u_{eq} = -f_n(\mathbf{x}) + \ddot{x}_c + k_1\dot{e} + k_2e \quad (9)$$

and the hitting controller  $u_{hr}$  is designed to guarantee the system stability as

$$u_{hr} = Z \operatorname{sgn}(s) \quad (10)$$

where  $\operatorname{sgn}(\cdot)$  is the sign function. Substituting (6), (7) and (8) into (6) yields

$$\ddot{e} + k_1\dot{e} + k_2e = -z - Z \operatorname{sgn}(s) = \dot{s}. \quad (11)$$

An important concept of sliding-mode control is to make the system satisfy the reaching condition and guarantee sliding condition. Consider the candidate Lyapunov function in the following form as

$$V = \frac{1}{2} s^2. \quad (12)$$

Differentiating (12) with respect to time and using (9) obtain

$$\begin{aligned} \dot{V}_1 &= s \dot{s} = -zs - Z|s| \\ &\leq |z||s| - Z|s| \\ &= -(Z - |z|)|s| \leq 0. \end{aligned} \quad (13)$$

In summary, the sliding-mode controller in (8) can guarantee the stability in the sense of the Lyapunov theorem [14]. However, large control gain  $Z$  is often required in order to minimize time needed to reach the switching surface from the initial state. A conservative control law with large control gain  $Z$  is usually considered, but unnecessary jumping movement between the switching surface may yield and cause an outcome of large amount of chattering. The chattering phenomena in control efforts will wear the bearing mechanism and excite unmodelled dynamics.

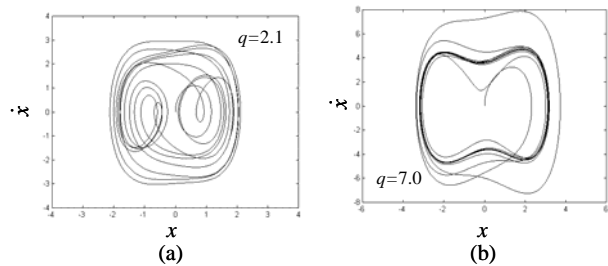


Fig. 1. Phase plane of uncontrolled chaotic dynamic system.

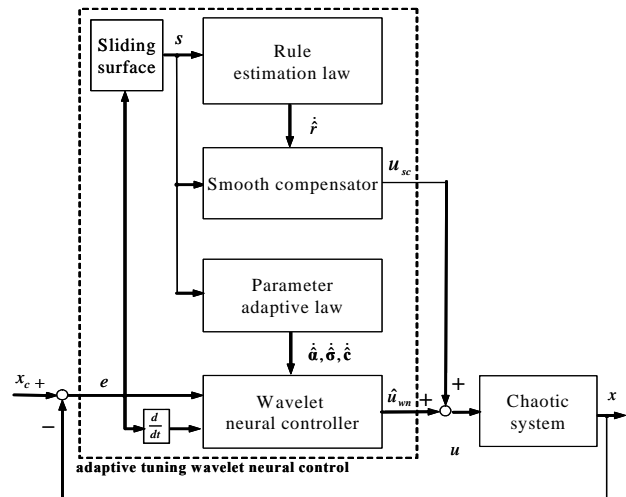


Fig. 2. ATWNC for chaotic system.

### III. ATWNC SYSTEM DESIGN

In this paper, the adaptive tuning wavelet neural control (ATWNC) system is proposed as shown in Fig. 2, where the controller output is defined as

$$u = \hat{u}_{wn} + u_{sc} \quad (14)$$

The wavelet neural controller  $\hat{u}_{wn}$  uses a WNN to approximate the ideal controller  $u^*$ , and the smooth compensator  $u_{sc}$  is utilized to compensate the approximation error between wavelet neural controller and ideal controller. The descriptions of design steps are depicted as follows:

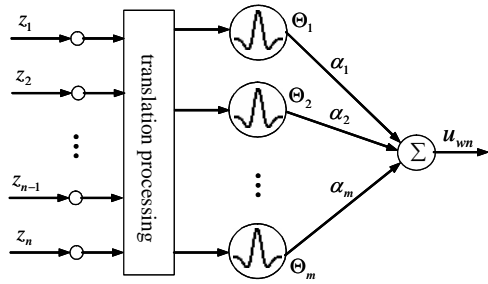


Fig. 3. Network structure of a wavelet neural network.

#### A. Description of WNN

The network structure of WNN is shown in Fig. 3, which can be considered as “1”-layer feedforward neural network with input preprocessing element. The WNN output with  $m$  wavelet basis functions can perform the mapping according to [9]

$$u_{wn} = \sum_{j=1}^m \alpha_j \Theta_j(\sigma_j, (\mathbf{z} - \mathbf{c}_j)) \quad (15)$$

where  $\mathbf{z} = [z_1 \ z_2 \ \dots \ z_n]^T$  is the input vector,  $\Theta_j(\sigma_j, (\mathbf{z} - \mathbf{c}_j))$ ,  $j = 1, 2, \dots, m$  are the wavelet functions,  $\sigma_j = [\sigma_{1j} \ \sigma_{2j} \ \dots \ \sigma_{nj}]^T$  and  $\mathbf{c}_j = [c_{1j} \ c_{2j} \ \dots \ c_{nj}]^T$  are the dilation and translation parameters, respectively,  $\alpha_j$  is the output layer weight. Each wavelet network's neuron in the translation layer can be represented by

$$\Theta_j = h_j(\mathbf{z}) \exp\left(-\sum_{k=1}^n \sigma_{kj}^2 (z_k - c_{kj})^2\right) \quad (16)$$

where the “Mexican hat” mother wavelet function is defined as  $h_j(\mathbf{z}) = \prod_{k=1}^n (1 - w_k^2 z_k^2)$ . For ease of notation, (15) can be expressed in a compact vector form as

$$u_{wn} = \mathbf{a}^T \Theta(\mathbf{z}, \boldsymbol{\sigma}, \mathbf{c}) \quad (17)$$

where  $\mathbf{a} = [\alpha_1 \ \alpha_2 \ \dots \ \alpha_m]^T$ ,  $\Theta = [\Theta_1 \ \Theta_2 \ \dots \ \Theta_m]^T$ ,  $\boldsymbol{\sigma} = [\sigma_1 \ \sigma_2 \ \dots \ \sigma_m]^T$  and  $\mathbf{c} = [c_1 \ c_2 \ \dots \ c_m]^T$ . This implies that there is a WNN of (17) that can uniformly approximate an ideal controller. There exists ideal weight vectors so that [9]

$$u^* = \mathbf{a}^{*T} \Theta^*(\mathbf{z}, \boldsymbol{\sigma}^*, \mathbf{c}^*) + \Delta \quad (18)$$

where  $\mathbf{a}^*$  and  $\Theta^*$  are optimal parameter vectors of  $\mathbf{a}$  and  $\Theta$ , respectively;  $\boldsymbol{\sigma}^*$  and  $\mathbf{c}^*$  are optimal parameter vectors of  $\boldsymbol{\sigma}$  and  $\mathbf{c}$ , respectively; and  $\Delta$  is the approximation error. However, the optimal parameter vectors are unknown, so it is necessary to estimate the values. Define an estimation

function

$$\hat{u}_{wn} = \hat{\mathbf{a}}^T \hat{\Theta}(\mathbf{z}, \hat{\boldsymbol{\sigma}}, \hat{\mathbf{c}}) \quad (19)$$

where  $\hat{\mathbf{a}}$  and  $\hat{\Theta}$  are optimal parameter vectors of  $\mathbf{a}$  and  $\Theta$ , respectively; and  $\hat{\boldsymbol{\sigma}}$  and  $\hat{\mathbf{c}}$  are optimal parameter vectors of  $\boldsymbol{\sigma}$  and  $\mathbf{c}$ , respectively. Define the estimation error as

$$\begin{aligned} \tilde{u} &= u^* - \hat{u}_{wn} = \mathbf{a}^{*T} \Theta^* - \hat{\mathbf{a}}^T \hat{\Theta} + \Delta \\ &= \tilde{\mathbf{a}}^T \tilde{\Theta} + \hat{\mathbf{a}}^T \tilde{\Theta} + \tilde{\mathbf{a}}^T \hat{\Theta} + \Delta \end{aligned} \quad (20)$$

where  $\tilde{\mathbf{a}} = \mathbf{a}^* - \hat{\mathbf{a}}$  and  $\tilde{\Theta} = \Theta^* - \hat{\Theta}$ . In order to deduce the adaptive law for mean and variance later, it is necessarily to derive the value of  $\tilde{\Theta}$ . To achieve this goal, the Taylor expansion linearization technique is employed to transform the nonlinear function into a partially linear form, such that [9]

$$\tilde{\Theta} = \mathbf{A}^T \tilde{\boldsymbol{\sigma}} + \mathbf{B}^T \tilde{\mathbf{c}} + \mathbf{h} \quad (21)$$

where  $\tilde{\boldsymbol{\sigma}} = \boldsymbol{\sigma}^* - \hat{\boldsymbol{\sigma}}$ ,  $\tilde{\mathbf{c}} = \mathbf{c}^* - \hat{\mathbf{c}}$ ,  $\mathbf{A} = \left[ \frac{\partial \Theta_1}{\partial \boldsymbol{\sigma}} \ \dots \ \frac{\partial \Theta_m}{\partial \boldsymbol{\sigma}} \right]_{\boldsymbol{\sigma}=\hat{\boldsymbol{\sigma}}}$ ,

$\mathbf{B} = \left[ \frac{\partial \Theta_1}{\partial \mathbf{c}} \ \dots \ \frac{\partial \Theta_m}{\partial \mathbf{c}} \right]_{\mathbf{c}=\hat{\mathbf{c}}}$ , and  $\mathbf{h}$  is the high order terms of expansion. Substitute (21) into (20), it can obtain that

$$\begin{aligned} \tilde{u} &= \tilde{\mathbf{a}}^T \tilde{\Theta} + \hat{\mathbf{a}}^T (\mathbf{A}^T \tilde{\boldsymbol{\sigma}} + \mathbf{B}^T \tilde{\mathbf{c}} + \mathbf{h}) + \tilde{\mathbf{a}}^T \hat{\Theta} + \Delta \\ &= \tilde{\mathbf{a}}^T \hat{\Theta} + \tilde{\boldsymbol{\sigma}}^T \mathbf{A} \hat{\mathbf{a}} + \tilde{\mathbf{c}}^T \mathbf{B} \hat{\mathbf{a}} + \hat{\mathbf{a}}^T \mathbf{h} + \tilde{\mathbf{a}}^T \tilde{\Theta} + \Delta \end{aligned} \quad (22)$$

where  $\hat{\mathbf{a}}^T \mathbf{A}^T \tilde{\boldsymbol{\sigma}} = \tilde{\boldsymbol{\sigma}}^T \mathbf{A} \hat{\mathbf{a}}$  and  $\hat{\mathbf{a}}^T \mathbf{B}^T \tilde{\mathbf{c}} = \tilde{\mathbf{c}}^T \mathbf{B} \hat{\mathbf{a}}$  are used since they are scalars. To speed up the convergence of WNN learning, the optimal parameter vector  $\mathbf{a}^*$  is decomposed into two parts as [4]

$$\mathbf{a}^* = \eta_p \mathbf{a}_p^* + \eta_i \mathbf{a}_i^* \quad (23)$$

where  $\eta_p$  and  $\eta_i$  are positive constants, and  $\mathbf{a}_p^*$  and  $\mathbf{a}_i^*$  are the proportional and integral terms of  $\mathbf{a}^*$ , respectively, and  $\mathbf{a}_i^* = \int_0^t \mathbf{a}_p^* d\tau$ . The estimation parameter vector  $\hat{\mathbf{a}}$  is decomposed into two parts as

$$\hat{\mathbf{a}} = \eta_p \hat{\mathbf{a}}_p + \eta_i \hat{\mathbf{a}}_i \quad (24)$$

where  $\hat{\mathbf{a}}_p$  and  $\hat{\mathbf{a}}_i$  are the proportional and integral terms of  $\hat{\mathbf{a}}$ , respectively, and  $\hat{\mathbf{a}}_i = \int_0^t \hat{\mathbf{a}}_p d\tau$ . Thus,  $\tilde{\mathbf{a}}$  can be expressed as

$$\tilde{\mathbf{a}} = \eta_i \tilde{\mathbf{a}}_i - \eta_p \hat{\mathbf{a}}_p + \eta_p \mathbf{a}_p^* \quad (25)$$

where  $\tilde{\mathbf{a}}_i = \mathbf{a}_i^* - \hat{\mathbf{a}}_i$ . Substituting (25) into (22) obtains

$$\begin{aligned} \tilde{u} &= (\eta_i \tilde{\mathbf{a}}_i - \eta_p \hat{\mathbf{a}}_p + \eta_p \mathbf{a}_p^*)^T \hat{\Theta} \\ &\quad + \tilde{\boldsymbol{\sigma}}^T \mathbf{A} \hat{\mathbf{a}} + \tilde{\mathbf{c}}^T \mathbf{B} \hat{\mathbf{a}} + \hat{\mathbf{a}}^T \mathbf{h} + \tilde{\mathbf{a}}^T \tilde{\Theta} + \Delta \\ &= \eta_i \tilde{\mathbf{a}}_i^T \hat{\Theta} - \eta_p \hat{\mathbf{a}}_p^T \hat{\Theta} + \tilde{\boldsymbol{\sigma}}^T \mathbf{A} \hat{\mathbf{a}} + \tilde{\mathbf{c}}^T \mathbf{B} \hat{\mathbf{a}} + \varepsilon \end{aligned} \quad (26)$$

where the uncertain term  $\varepsilon = \eta_p \mathbf{a}_p^{*T} \hat{\Theta} + \hat{\mathbf{a}}^T \mathbf{h} + \tilde{\mathbf{a}}^T \tilde{\Theta} + \Delta$ .

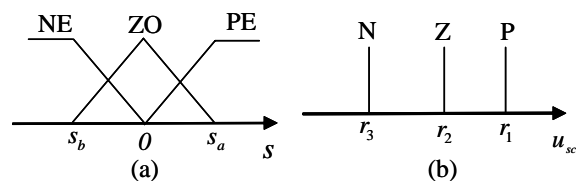


Fig. 4. (a) input fuzzy sets. (b) output fuzzy sets.

### B. Smooth compensator

Assume that the smooth compensator has 3 fuzzy rules in a rule base as given in the following form [16]

Rule 1: If  $s$  is PE, then  $u_{sc}$  is P (27)

Rule 2: If  $s$  is ZO, then  $u_{sc}$  is Z (28)

Rule 3: If  $s$  is NE, then  $u_{sc}$  is N (29)

where the triangular-typed functions and singletons are used to define the membership functions of IF-part and THEN-part, which are depicted in Figs. 4(a) and 4(b), respectively. The defuzzification of the output is accomplished by the method of center-of-gravity

$$u_{sc} = \frac{\sum_{i=1}^3 r_i w_i}{\sum_{i=1}^3 w_i} = r_1 w_1 + r_2 w_2 + r_3 w_3 \quad (30)$$

where  $0 \leq w_1 \leq 1$ ,  $0 \leq w_2 \leq 1$  and  $0 \leq w_3 \leq 1$  are the firing strengths of rules 1, 2, and 3, respectively; and the relation  $w_1 + w_2 + w_3 = 1$  is valid according to the special case of triangular membership function-based fuzzy system. In order to reduce the computation loading, let  $r_1 = \hat{r}$ ,  $r_2 = 0$  and  $r_3 = -\hat{r}$ . Hence, for any value of input  $x$ , only one of four conditions will occur according to Fig. 4(a) as [17]

Condition1: Only rule 1 is triggered ( $x > x_a$ ,  $w_1 = 1$ ,  $w_2 = w_3 = 0$ )

$$u_{sc} = r_1 = \hat{r} \quad (31)$$

Condition2: Rules 1 and 2 are triggered simultaneously. ( $0 < x \leq x_a$ ,  $0 < w_1, w_2 \leq 1$ ,  $w_3 = 0$ )

$$u_{sc} = r_1 w_1 = \hat{r} w_1 \quad (32)$$

Condition3: Rules 2 and 3 are triggered simultaneously. ( $x_b < x \leq 0$ ,  $w_1 = 0$ ,  $0 < w_2, w_3 \leq 1$ )

$$u_{sc} = r_3 w_3 = -\hat{r} w_3 \quad (33)$$

Condition 4: Only rule 3 is triggered. ( $x \leq x_b$ ,  $w_1 = w_2 = 0$ ,  $w_3 = 1$ )

$$u_{sc} = r_3 = -\hat{r} \quad (34)$$

Then, the (31)-(34) can be rewritten as

$$u_{sc} = \hat{r}(w_1 - w_3) \quad (35)$$

Moreover, it can see that [17]

$$s(w_1 - w_3) = |s| |(w_1 - w_3)| \geq 0 \quad (36)$$

### C. On-line learning algorithm

Substituting (10) into (7) and using (8), yields

$$\ddot{e} + k_1 \dot{e} + k_2 e = u^* - \hat{u}_{wn} - u_{sc} = \dot{s} \quad (37)$$

By using the approximation property (26), (37) can be rewritten as

$$\dot{s} = \eta_l \tilde{\mathbf{a}}_1^T \hat{\Theta} - \eta_p \hat{\mathbf{a}}_1^T \hat{\Theta} + \tilde{\sigma}^T \mathbf{A} \hat{\mathbf{u}} + \tilde{\mathbf{c}}^T \mathbf{B} \hat{\mathbf{u}} + \varepsilon - u_{sc} \quad (38)$$

To proof the stability of the ATWNC system, define a Lyapunov function candidate in the following form

$$V_a = \frac{1}{2} s^2 + \frac{\eta_l}{2} \tilde{\mathbf{a}}_1^T \tilde{\mathbf{a}}_1 + \frac{1}{2\eta_\sigma} \tilde{\sigma}^T \tilde{\sigma} + \frac{1}{2\eta_c} \tilde{\mathbf{c}}^T \tilde{\mathbf{c}} \quad (39)$$

where  $\eta_\sigma$  and  $\eta_c$  are the learning rates with positive constants. Differentiating (39) with respect to time and using (38), it is obtained that

$$\begin{aligned} \dot{V}_a &= s\dot{s} + \eta_l \tilde{\mathbf{a}}_1^T \dot{\tilde{\mathbf{a}}}_1 + \frac{1}{\eta_\sigma} \tilde{\sigma}^T \dot{\tilde{\sigma}} + \frac{1}{\eta_c} \tilde{\mathbf{c}}^T \dot{\tilde{\mathbf{c}}} \\ &= \eta_l \tilde{\mathbf{a}}_1^T (s\hat{\Theta} + \dot{\tilde{\mathbf{a}}}_1) + \tilde{\sigma}^T (s\mathbf{A}\hat{\mathbf{u}} + \frac{\dot{\tilde{\sigma}}}{\eta_\sigma}) + \tilde{\mathbf{c}}^T (s\mathbf{B}\hat{\mathbf{u}} + \frac{\dot{\tilde{\mathbf{c}}}}{\eta_c}) \\ &\quad - s\eta_p \hat{\mathbf{a}}_1^T \hat{\Theta} + s(\varepsilon - u_{sc}) \end{aligned} \quad (40)$$

If the parameter adaptive laws are selected as

$$\dot{\hat{\mathbf{a}}}_p = s\hat{\Theta} \quad (41)$$

$$\dot{\tilde{\mathbf{a}}}_1 = -\dot{\tilde{\mathbf{a}}}_1 = s\hat{\Theta} \quad (42)$$

$$\dot{\tilde{\sigma}} = -\dot{\tilde{\sigma}} = \eta_\sigma s\mathbf{A}\hat{\mathbf{u}} \quad (43)$$

$$\dot{\tilde{\mathbf{c}}} = -\dot{\tilde{\mathbf{c}}} = \eta_c s\mathbf{B}\hat{\mathbf{u}} \quad (44)$$

and the smooth compensator is design as (35), then (40) can be rewritten as

$$\begin{aligned} \dot{V}_a &= -\eta_p \hat{\mathbf{a}}_p^T \hat{\mathbf{a}}_p + s(\varepsilon - u_{sc}) \\ &\leq -\eta_p \hat{\mathbf{a}}_p^T \hat{\mathbf{a}}_p + |s| |\varepsilon| - \hat{r} s(w_1 - w_3) \\ &\leq |s| |\varepsilon| - \hat{r} |s| |w_1 - w_3| \\ &= -|s| |w_1 - w_3| \left( \hat{r} - \frac{|\varepsilon|}{|w_1 - w_3|} \right) \end{aligned} \quad (45)$$

If the following inequality

$$\hat{r} > \frac{|\varepsilon|}{|w_1 - w_3|} \quad (46)$$

holds, then the sliding condition  $\dot{V}_a \leq 0$  can be satisfied.

Owing to the unknown lumped uncertainties, the value  $\hat{r}$  cannot be exactly obtained in advance for practical applications. According to (46), there exists an ideal value  $r^*$  as follows to achieve minimum value and match the sliding condition:

$$r^* = \frac{|\varepsilon|}{|w_1 - w_3|} + \kappa \quad (47)$$

where  $\kappa$  is a positive constant. Thus, a simple adaptive algorithm is utilized in this study to estimate the ideal value of  $r^*$ , and its estimated error is defined as

$$\tilde{r} = r^* - \hat{r} \quad (48)$$

where  $\hat{r}$  is the estimated value of the optimal value of  $r^*$ . Then, define a new Lyapunov function candidate in the following form

$$V_b = \frac{1}{2} s^2 + \frac{\eta_l}{2} \tilde{\mathbf{a}}_1^T \tilde{\mathbf{a}}_1 + \frac{1}{2\eta_\sigma} \tilde{\sigma}^T \tilde{\sigma} + \frac{1}{2\eta_c} \tilde{\mathbf{c}}^T \tilde{\mathbf{c}} + \frac{1}{2\eta_r} \tilde{r}^2 \quad (49)$$

where  $\eta_r$  is the learning rate with a positive constant. Differentiating (49) with respect to time and using (38) and (41)-(44), it is obtained that

$$\begin{aligned} \dot{V}_b &= s\dot{s} + \eta_l \tilde{\mathbf{a}}_1^T \dot{\tilde{\mathbf{a}}}_1 + \frac{1}{\eta_\sigma} \tilde{\sigma}^T \dot{\tilde{\sigma}} + \frac{1}{\eta_c} \tilde{\mathbf{c}}^T \dot{\tilde{\mathbf{c}}} + \frac{1}{\eta_r} \tilde{r} \dot{\tilde{r}} \\ &= -\eta_p \hat{\mathbf{a}}_p^T \hat{\mathbf{a}}_p + s\varepsilon - \hat{r} s(w_1 - w_3) + \frac{1}{\eta_r} \tilde{r} \dot{\tilde{r}} \\ &\leq s\varepsilon - \hat{r} s(w_1 - w_3) + \frac{1}{\eta_r} \tilde{r} \dot{\tilde{r}} \\ &\leq |s| |\varepsilon| - \hat{r} s(w_1 - w_3) + r^* s(w_1 - w_3) - r^* s(w_1 - w_3) + \frac{1}{\eta_r} \tilde{r} \dot{\tilde{r}} \end{aligned}$$

$$\begin{aligned}
 &= |s|\|\varepsilon\| + \tilde{r}s(w_1 - w_3) - r^*s(w_1 - w_3) + \frac{1}{\eta_r} \tilde{r}\dot{\tilde{r}} \\
 &= \tilde{r}[s(w_1 - w_3) + \frac{1}{\eta_r} \dot{\tilde{r}}] + |s|\|\varepsilon\| - r^*|s|w_1 - w_3
 \end{aligned} \quad (50)$$

Choose the rule estimation laws as

$$\dot{\tilde{r}} = -\hat{r} = -\eta_r s(w_1 - w_3) \quad (51)$$

and using (47), (50) becomes

$$\begin{aligned}
 \dot{V}_b &= |s|\|\varepsilon\| - |s|(|\varepsilon| + \kappa|w_1 - w_3|) \\
 &= -\kappa|s|w_1 - w_3 \leq 0
 \end{aligned} \quad (52)$$

As a result, the stability of the proposed ATWNC system can be guaranteed.

#### IV. SIMULATION RESULTS

Chaotic system is a nonlinear deterministic system that displays complex, noisy-like and unpredictable behavior. It can be observed in many nonlinear circuits and mechanical systems. For control engineers, control of a chaotic system has become a significant research topic in physics, mathematics and engineering communities. The simulation results of the chaotic system are presented here to verify the effectiveness of the proposed ATWNC scheme. It should be emphasized that the derivation of ATWNC do not need to know the system dynamic function. The proposed ATWNC is applied to chaotic dynamic system again. The control parameters are selected as  $k_1 = 2$ ,  $k_2 = 1$ ,  $\eta_l = \eta_p = 20$  and  $\eta_\sigma = \eta_c = 1$ . All the gains in the ATWNC are chosen to achieve good transient control performance in the simulation considering the requirement of stability and possible operating conditions. As  $\eta_p = 0$ , the learning algorithm of the proposed method is the same as conventional WNN-based adaptive control. The simulation results of ATWNC with  $\eta_p = 0$  for  $q = 2.1$  and  $q = 7.0$  are shown in Fig. 5. The tracking responses of state  $x$  are shown in Figs. 5(a) and 5(d); the tracking responses of state  $\dot{x}$  are shown in Figs. 5(b) and 5(e); and the associated control efforts are shown Figs. 5(c) and 5(f) for  $q = 2.1$  and  $q = 7.0$ , respectively. The simulation results show that it can achieve favorable tracking performance; however, the convergence of controller parameter and tracking error is slow. Moreover, to achieve faster convergence performance,  $\eta_p = 20$  is reconsidered. The simulation results of ATWNC with  $\eta_p = 20$  for  $q = 2.1$  and  $q = 7.0$  are shown in Fig. 6. The tracking responses of state  $x$  are shown in Figs. 6(a) and 6(d); the tracking responses of state  $\dot{x}$  are shown in Figs. 6(b) and 6(e); and the associated control efforts are shown Figs. 6(c) and 6(f) for  $q = 2.1$  and  $q = 7.0$ , respectively. From the simulation results, it is seen that the convergence of controller parameter and tracking error converge quickly.

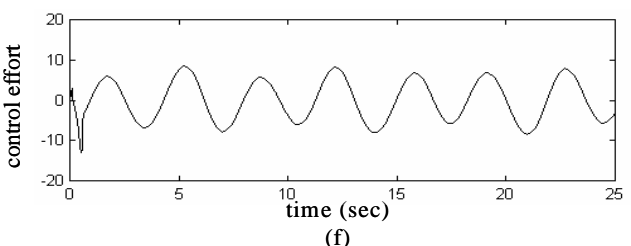
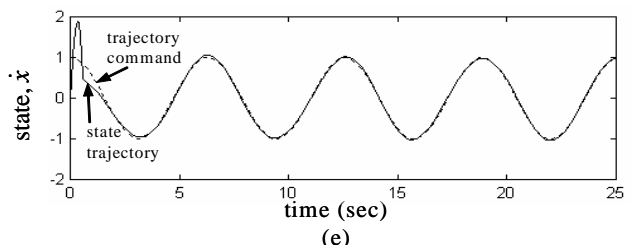
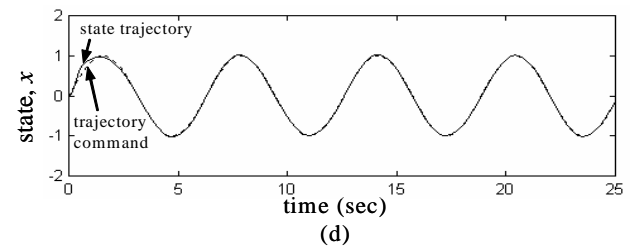
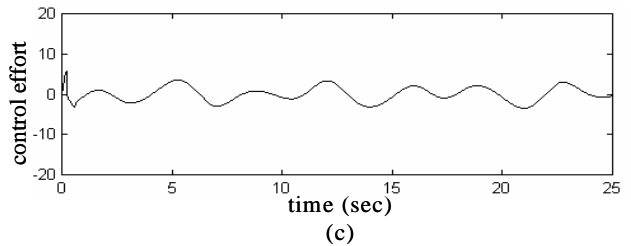
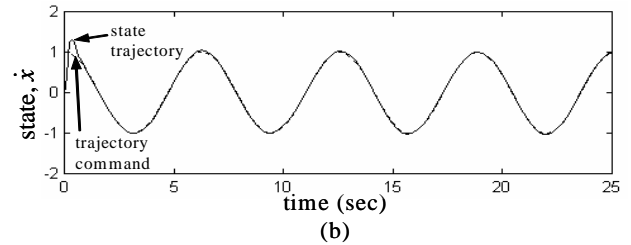
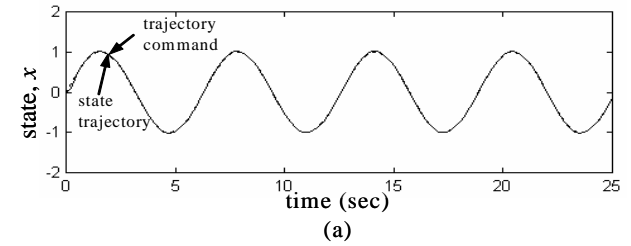
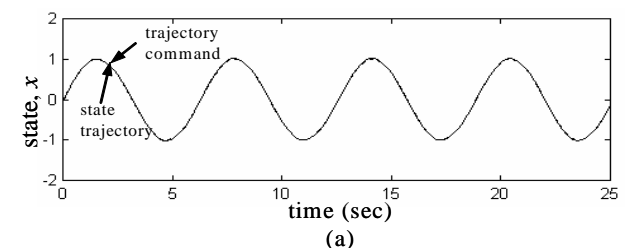


Fig. 5. Simulation results of ATWNC with  $\eta_p = 0$ .



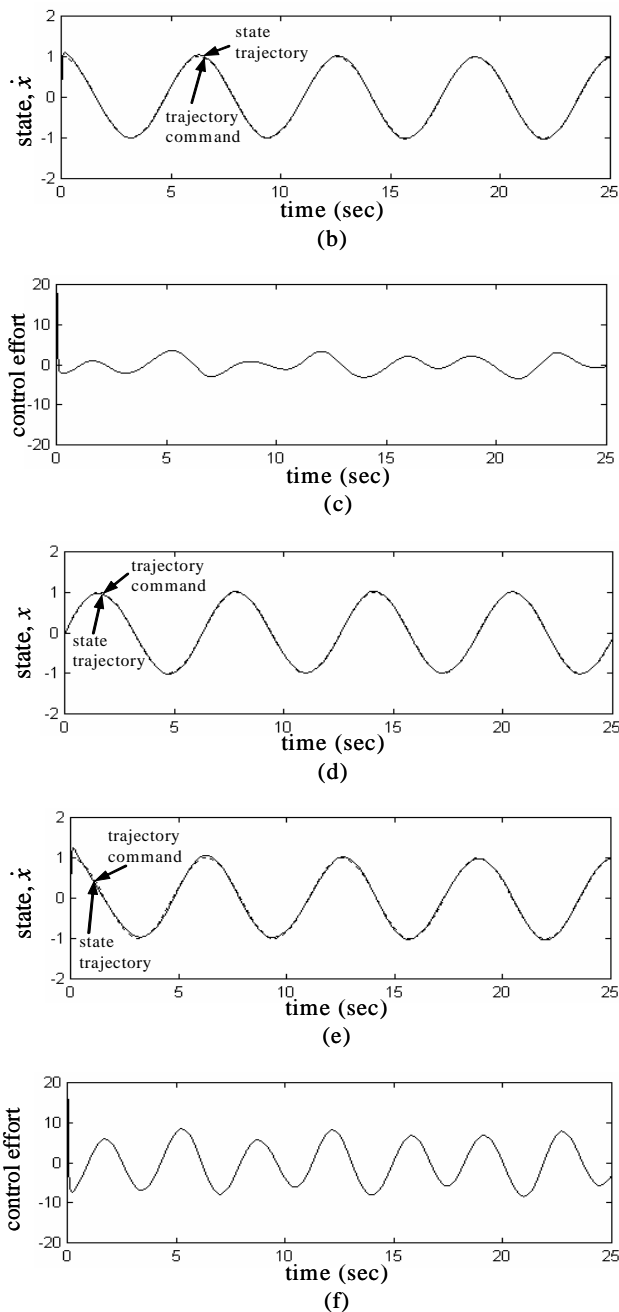


Fig. 6. Simulation results of ATWNC with  $\eta_p = 20$ .

## V. CONCLUSIONS

An adaptive tuning wavelet neural control (ATWNC) with a PI type learning algorithm is proposed for a chaotic dynamic system. The stability is proven by Lyapunov function with the online parameter tuning laws are given to adjust the interconnection weights, dilation and translation parameters of wavelet functions. The effectiveness of the ATWNC system is verified by some simulations. The main contributions of this paper are: (1) a learning algorithm with PI adaptation learning algorithm can achieve better tracking performance; and (2) the smooth compensator design uses a simple fuzzy system can remove completely the chattering phenomena.

## ACKNOWLEDGMENT

The authors appreciate the partial financial support from the National Science Council of Republic of China under grant NSC 97-2221-E-216-029.

## REFERENCES

- [1] S. A. Billings and H. L. Wei, "A new class of wavelet networks for nonlinear system identification," *IEEE Trans. Neural Netw.*, vol. 16, no. 4, 2005, pp. 862-874.
- [2] B. S. Chen and C. H. Chen, " $H^\infty$  tracking design of uncertain nonlinear SISO systems: adaptive fuzzy approach," *IEEE Trans. Fuzzy Syst.*, vol. 4, no. 1, 1996, pp. 32-43.
- [3] G. Chen and X. Dong, "On Feedback Control of Chaotic Continuous-Time Systems," *IEEE Trans. Circuits Syst. I*, vol. 40, no. 9, 1993, pp. 591-601.
- [4] N. Golea, A. Golea, and K. Benmahammed, "Fuzzy model reference adaptive control," *IEEE Trans. Fuzzy Syst.*, vol. 10, no. 4, 2002, pp. 436-444.
- [5] C. F. Hsu, C. M. Lin, and T. Y. Chen, "Neural-network-identification-based adaptive control of wing rock motion," *IEE Proc., Contr. Theory Appl.*, vol. 152, no.1, 2005, pp. 65-71.
- [6] C. F. Hsu, C. M. Lin, and T. T. Lee, "Wavelet adaptive backstepping control for a class of nonlinear systems," *IEEE Trans. Neural Netw.*, vol. 17, no. 5, 2006, pp. 1175-1183.
- [7] J. Q. Huang and F. L. Lewis, "Neural-network predictive control for nonlinear dynamic systems with time-delay," *IEEE Trans. Neural Netw.*, vol. 14, no. 2, 2003, pp. 377-389.
- [8] Z. P. Jiang, "Advanced feedback control of the chaotic Duffing equation," *IEEE Trans. Circuits Syst. I*, vol. 49, no. 2, 2002, pp. 244-249.
- [9] C. K. Lin, "Adaptive tracking controller design for robotic systems using Gaussian wavelet networks," *IEE Proc., Contr. Theory Appl.*, vol. 149, no. 4, 2002, pp. 316-322.
- [10] C. M. Lin and C. F. Hsu, "Neural network hybrid control for antilock braking systems," *IEEE Trans. Neural Netw.*, vol. 14, no. 2, 2003, pp. 351-359.
- [11] A. Loría and A. Zavala-Río, "Adaptive tracking control of chaotic systems with applications to synchronization," *IEEE Trans. Circuits Syst., I*, vol. 54, no. 9, 2007, pp. 2019-2029.
- [12] O. Omidvar and D. L. Elliott, *Neural Systems for Control*, Academic Press 1997.
- [13] J. H. Park, S. J. Seo, and G. T. Park, "Robust adaptive fuzzy controller for nonlinear system using estimation of bounds for approximation errors," *Fuzzy Set Syst.*, vol. 133, no. 1, 2003, pp. 19-36.
- [14] J. J. E. Slotine and W. P. Li, *Applied Nonlinear Control*, Englewood Cliffs, NJ: Prentice Hall, 1991.
- [15] C. D. Sousa, E. M. Hemerly, and R. K. H. Galvao, "Adaptive control for mobile robot using wavelet networks," *IEEE Trans. Syst., Man and Cybern., Pt B*, vol. 32, no. 4, 2002, pp. 493-504.
- [16] J. R. Timothy, *Fuzzy Logic with Engineering Application*. NewYork: Mc-Graw Hill, 1995.
- [17] R. J. Wai, "Fuzzy sliding-mode control using adaptive tuning technique," *IEEE Trans. Industrial Electronics*, vol. 54, no. 1, 2007, pp. 586-594.
- [18] H. Wang and Y. Wang, "Neural-network-based fault-tolerant control of unknown nonlinear systems," *IEE Proc., Contr. Theory Appl.*, vol. 146, no. 5, 1999, pp. 389-398.
- [19] W. Y. Wang, M. L. Chan, C. C. J. Hsu, and T. T. Lee, " $H^\infty$  tracking-based sliding mode control for uncertain nonlinear systems via an adaptive fuzzy-neural approach," *IEEE Trans. Syst., Man and Cybern., Pt B*, vol. 32, no. 4, 2002, pp. 483-492.
- [20] Q. Zhang, "Using wavelet network in nonparametric estimation," *IEEE Trans. Neural Netw.*, vol. 8, no. 2, 1997, pp. 227-236.